6th Australasian Hydraulics and
Fluid Mechanics Conference
Adelaide, Australia, 5-9 December 1977

# Choked Flow in a Jet Screen Configuration due to Cavitation

R. K. DUGGINS
Professor of Mechanical Engineering, Faculty of Military Studies, University of New South Wales

SUMMARY An experimental investigation has been performed to study the various stages of cavitation development in the radially outward flow of a jet screen configuration. Detailed measurements were made of discharge and static pressure and from these it has been possible to clarify inception phenomena and to determine for various sizes of gap the minimum value of the pressure ratio across the device for cavitation avoidance. Some unexpected aspects of cavitating discharge performance were also revealed.

## 1 INTRODUCTION

The geometry under consideration occurs in many types of control valve and is shown at the bottom of Fig. 1. It comprises a round jet discharging from a nozzle and then flowing radially outwards through a narrow gap between two parallel surfaces. Local pressures just inside the gap are lower than those at exit and this feature means that cavitation occurs when a large pressure difference is applied to the device. The flow separates at the sharp corner at the entrance to the gap, and then contracts. It is at the vena contracta section where the minimum pressure exists and accordingly it is here that the first signs of cavitation are observed, when the local pressure falls to the vapour pressure $P_v$ of the liquid. Further reduction of the downstream pressure $P_2$ extends the cavitating region and may cause the flow to become choked.

As the figures show, the parallel surfaces which confine the flow are called the land and the plate, the length L of the land clearly being an important dimension like the gap size x and the nozzle diameter D. To a large degree it is the x/L ratio which determines the nature of the radially outward flow and, in particular, whether the initially separated flow reattaches to the land (fully, partially or not at all) and whether additional separation occurs near the exit of the gap. Another important geometrical parameter is the x/D ratio since this is a measure of the relative effects of the gap and the nozzle in controlling the flowrate. (The circumferential (curtain) area at the entry to the gap is $\pi Dx$, the nozzle area is $\pi D^2/4$ and their ratio is $4x/D$). Here we are concerned only with the case where the gap effect is dominant so the appropriate definitions of discharge coefficient $C_D$ and $R_e$ are respectively:-

$$Q = C_D(\pi Dx)\sqrt{2(P_2-P_1)/\rho} \quad \text{and}$$

$$R_e = (Q/\pi Dx).x/\nu = Q/\pi\nu D.$$

## 2 REVIEW OF PREVIOUS WORK

Most of the previous work on this type of device has been for non-cavitating flows and for configurations where the gap was small both in width and radial extent. Such an investigation was made by Lichtarowicz [1] and Fig. 1 illustrates his results which were for particularly small values of the x/D ratio (max. x/D = 0.101). The x/L ratio was the governing geometrical parameter although its effect on discharge performance proved to be complicated and no consistent trend was observed with progressive increase in x/L up to the maximum value considered (0.88). At higher flowrates ($R_e > 2000$), $C_D$ was found to be relatively insensitive to changes in $R_e$.

The corresponding results for x/L = 0.55 are shown in the lower part of the figure and, unlike the previously discussed data, reveal a flow instability which was manifest as a sudden change in the value of $C_D$ (a 15% change at $R_e \simeq 1800$). Cavitation occurred at $R_e \simeq 2200$. Although the discharge was thereafter more variable, the cavitation was surprisingly not accompanied by any consistent reduction in $C_D$. The majority of the work was carried out with a small nozzle (D = 2 mm), and gap sizes as low as 0.032 mm were employed.

The results of Biryukov [2], intended primarily to clarify cavitation inception, are shown in Fig. 2. Typical discharge characteristics are indicated by the broken lines at the top of the figure and relate to a particular configuration in which the nozzle pressure $P_G$ was maintained at different levels. The points of inflexion at A and B indicate inception and the vertical lines below the points indicate choking of the flow, and constant discharge with further reduction of $P_2$. Clearly there is a major conflict between these results for cavitating flow and the corresponding data given by Lichtarowicz (for x/L = 0.55) which show that the performance was not noticeably different from that for non-cavitating flow. Biryukov indicates that, for similar x/L ratios, cavitation caused choking in every case and the flowrate afterwards remained constant. In addition, the change in performance is reported to have been surprisingly rapid and manifest as a sudden change in the gradient of the discharge characteristic.

The continuous curves shown in Fig. 2 define the boundaries between non-cavitating flows (above the lines) and cavitating ones (below). As with the discharge characteristics of Fig. 1, the curves do not exhibit any consistent trend regarding the effects of x/L, x/D and $R_e$ on inception although, as expected, the larger x/D and x/L values were generally associated with smaller critical pressure ratios $P_2^*/P_G$. The situation is confused by the fact that the x/D values were relatively large (implying that the nozzle constricted the flow significantly) and the $R_e$ range was low (max. $R_e$ = 350) indicating

that the flow was probably $R_e$ dependent too. The largest nozzle used in the tests had a diameter of 1.2 mm.

## 3 DISCUSSION OF RESULTS

The primary objective has been to extend the previous work by examining a wider range of configurations and by studying the cavitation phenomena in greater detail. A schematic diagram of the test rig is given in Fig. 3 and attention is drawn to the fact that the main elements of the device were much larger than those used in the previous investigations. (D = 30 mm, L = 30 mm and the moveable plate could be positioned to give gaps up to 5 mm in width). The long land will be shown to have yielded a more stable flow and a more consistent discharge performance. The wide gap meant that (a) its size could be accurately set, (b) tests could be performed at large values of $R_e$ (typically $3 \times 10^4$) where the performance was relatively insensitive to $R_e$ changes and (c) sufficient tappings could be accommodated along the land to enable distributions of static pressure to be obtained in some detail. Eleven tappings were used, each 0.8 mm in diameter, and they were positioned along a spiral contour as shown in the figure. Water was used as the working fluid and no attempt was made to control its air content in view of the previous findings [3] that the concentration of dissolved gas has little effect on cavitation.

A selection of discharge results is given in Fig. 4 for gap widths of 1, 2, 3 and 4 mm corresponding to equal x/L and x/D ratios of 0.033, 0.067, 0.100 and 0.133 respectively. Reflecting a stable physical situation, the experimental points define the discharge characteristics with very little scatter for both cavitating and non-cavitating flows, each curve having been obtained by holding $P_1$ constant and varying $P_2$ - the same practice that had been adopted by Biryukov.

Presentation of the data in the form Q vs $\sqrt{P_1 - P_2}$ results in the non-cavitating flow data appearing in the figure as a family of inclined straight lines. Their gradients are approximately in proportion to the corresponding widths of the gap and enable the $C_D$ values associated with single phase, incompressible conditions to be calculated. The first indications of cavitation inception were audible ones, initially in the form of a whistle, and a further small reduction in $P_2$ then caused the performance to begin to deviate from the inclined straight line characteristic.

It is this part of the data which throws light on the conflict of evidence apparent in the previous work. Once cavitation inception had occurred, the characteristic almost immediately became horizontal indicating a choked flow with no further increase in Q. In fact closer examination of the figure reveals that in each case the magnitude of $\hat{Q}$ was approximately proportional to $\sqrt{P_1}$ and this was to be expected since the controlling downstream pressure was no longer $P_2$ but $P_v$ at the point of minimum pressure. The governing pressure differential across the device was therefore $(P_1 - P_v)$ and approximately $P_1$ alone since $P_v$ was very small. The constants of proportionality in the $\hat{Q}$ vs $\sqrt{P_1}$ relationships are again approximately in proportion to the gap widths and correspond to a $C_{DC}$ value of a little over 0.7 in the equation $\hat{Q} = C_{DC}(\pi Dx)\sqrt{2P_1/\rho}$. It is somewhat higher, therefore, than the value of 0.61 known to apply in the case of choked cavitating flow through a short pipe. (An alternative parameter which has been employed by some investigators is a "Cavitation number $\sigma$" which is related to $C_{DC}$ by the expression $\sigma = C_{DC}^{-2}$). Although the ranges of x/L and $R_e$ are different from those considered by Biryukov, it may be concluded that the results are broadly in agreement both for non-cavitating flows and for cavitating flows just after inception.

The agreement also extends to the inception condition itself, defined by the intersection point of the inclined and the horizontal straight lines of each characteristic. The critical values of $P_2$, say $P_2^*$, are found to be approximately constant fractions of the corresponding $P_1$ values, the ratio $P_2^*/P_1$ having average values of 0.73, 0.64 and 0.57 for 1, 2 and 3 mm gaps respectively. (For the 4 mm gap, supply limitations meant that insufficient data were available to define the critical pressure ratio in this case.) The three values of the ratio are higher than Biryukov's (probably due to the smaller x/L ratios) although their descending magnitudes with increasing gap size follow the same pattern. One might also expect $P_2^*/P_1$ and $C_D$ to be related by the expression $C_{DC}\sqrt{P_1} = C_D\sqrt{P_1 - P_2^*}$ since the coordinates of the point of intersection must satisfy the equations of both straight lines. The equation can be written in the alternative form $P_2^*/P_1 = 1 - (C_{DC}/C_D)^2$ and since $C_{DC}^2 \simeq 0.5$, it may be further reduced to $P_2^*/P_1 \simeq 1 - 0.5C_D^{-2}$. So far, insufficient data have been obtained to validate this but additional work is in progress with the object of doing so. No consistent $R_e$ effect was observed in the inception phenomena, indicating that the flowrates were sufficiently large for operation to be in the regime of $R_e$ independence.

In previous experimentation using different geometrical configurations it was found that, although cavitation inception was clearly defined, the point of desinence (the disappearance of choked cavitation when the pressure ratio was increased again) was more variable and instances of desinence delay were recorded. However, in the present investigation "hysteresis" was observed in only one test (x = 2 mm, $P_1$ = 4 bar (a)), and could not readily be reproduced. The explanation for its virtual absence in the geometry of the radially outward flow may be that the region of minimum pressure, where the choked cavitation was believed to start and later to disappear, extended all round the nozzle, the circumferential length of the region having been about 100 mm in the present rig.

Another interesting feature of the discharge characteristics, particularly evident at high $P_1$ values for x = 1 mm, was that reduction of $P_2$ to levels much lower than for cavitation inception (typically $P_2 \simeq P_2^*/2$) caused Q to fall by up to 10% from its previously constant value. Even lower $P_2$ values then caused the discharge to stabilise or partially recover. One can only speculate why the performance changed in this way and, in particular, why the increasing pressure difference across the device was accompanied by a decrease in flowrate.

Turning now to the measurements of static pressure along the land, it will be recalled that they were obtained with tappings distributed along a spiral line rather than along a radial one. This needs to be borne in mind because the flow through the device (and the pressure distribution too) was probably asymmetric, with separation having occurred in one angular position but not another, so that some of the measured profiles may differ from corresponding distributions along a particular radial flow-path. Fig. 5 depicts two families of curves, representing different stages of cavitation development, and

relate to a gap size of 1 mm. The full lines are for $P_1$ = 4 bar(a) and for various levels of $P_2$ both above and below the corresponding critical value of approximately 3 bar(a); the broken lines are for $P_1$ = 9 bar(a), $P_2$* in this case being about 7 bar(a).

The profiles were essentially similar in shape, whether the flow was cavitating or not and surprisingly the previously described abrupt changes in discharge characteristic at inception were not accompanied by any corresponding changes in the pressure distributions. Each curve comprised a low pressure region at the entrance to the gap, a large and rapid pressure rise in the flow reattachment region and, in the case of the smaller flows, a further small recovery as the gap exit was approached. For the cavitating flows, the measured pressure at the entrance were approximately 0.1 bar(a) and such differences in profile shape as there were occurred in the location of reattachment. Progressive reduction of $P_2$ caused the low pressure region to extend radially outwards, indicating a spreading of the cavitation, and when $P_2/P_1$ had fallen to about 0.25 the cavitation virtually filled the gap with the flow in effect remaining detached from the walls. The wall pressure was then approximately constant everywhere and equal to 0.1 bar(a). For the non-cavitating flows, the entry pressure was higher of course and the reattachment occurred in a shorter length.

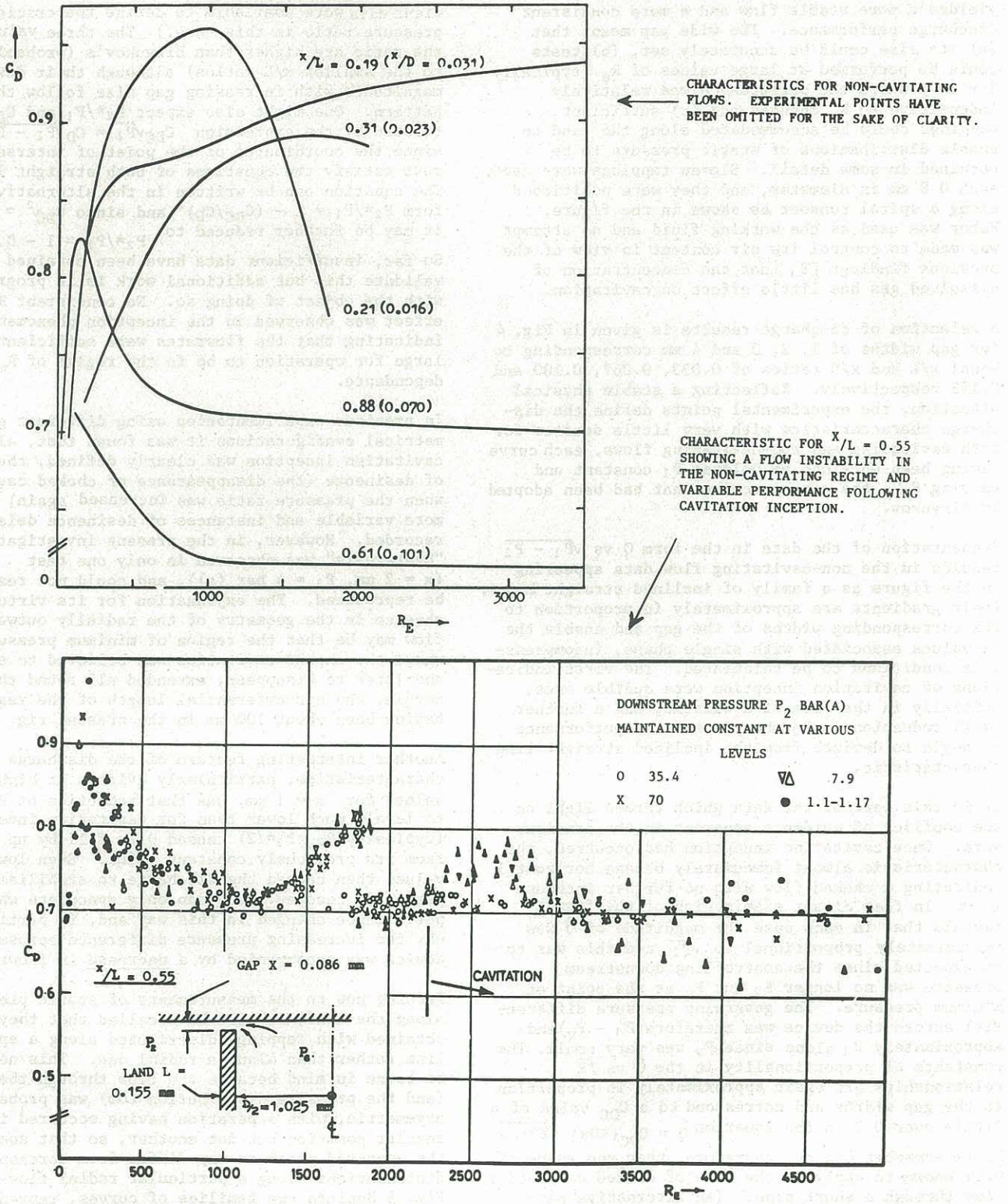


Figure 1 Discharge characteristics for a jet screen device having a very small land dimension. (Lichtarowicz and Lorimer)

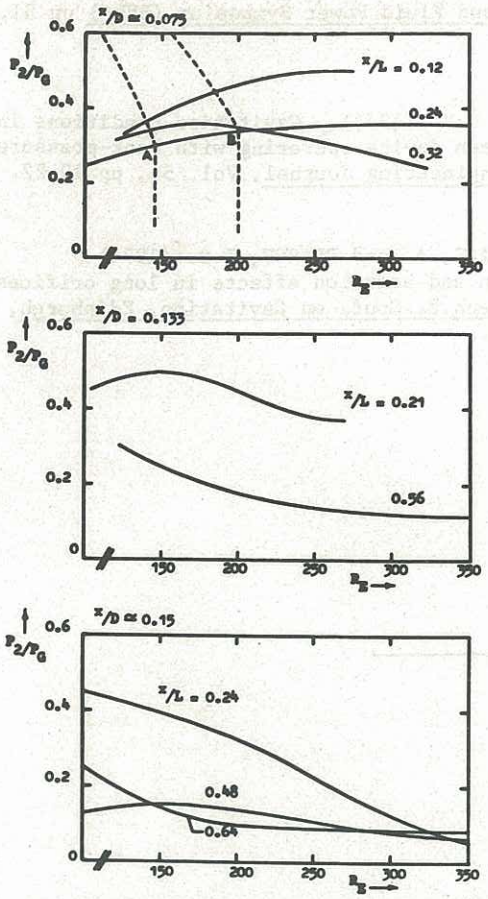


Figure 2 Cavitation inception boundaries (Biryukov)

The curves define the boundaries between non-cavitating flows (above the lines) and cavitating ones (below).

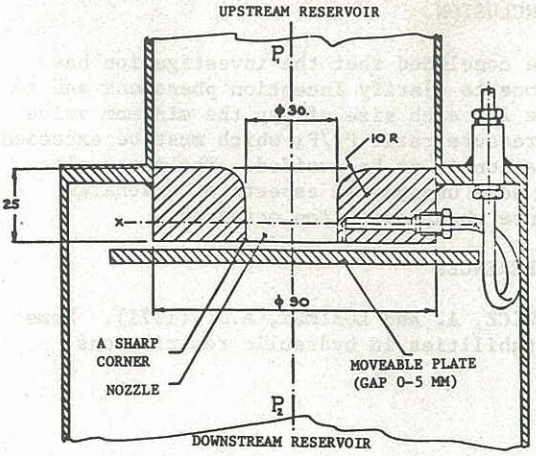


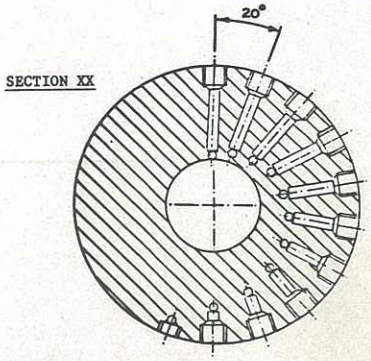


Figure 3 Schematic diagram of the present test arrangement

There are eleven pressure tappings 0.8 mm dia. at 20° intervals and at progressively increasing radius. All dimensions are in millimetres.

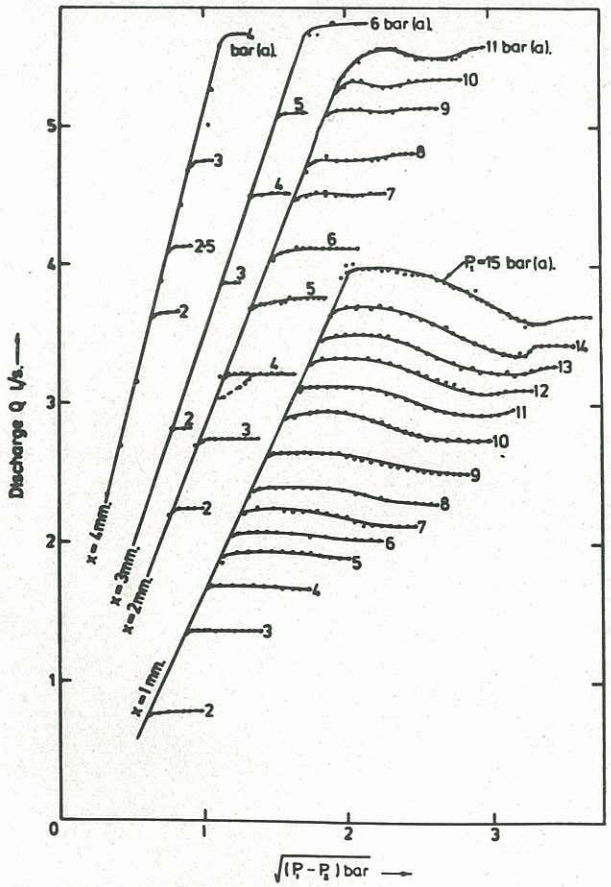


Figure 4 Discharge characteristics for various gap sizes and upstream pressures.

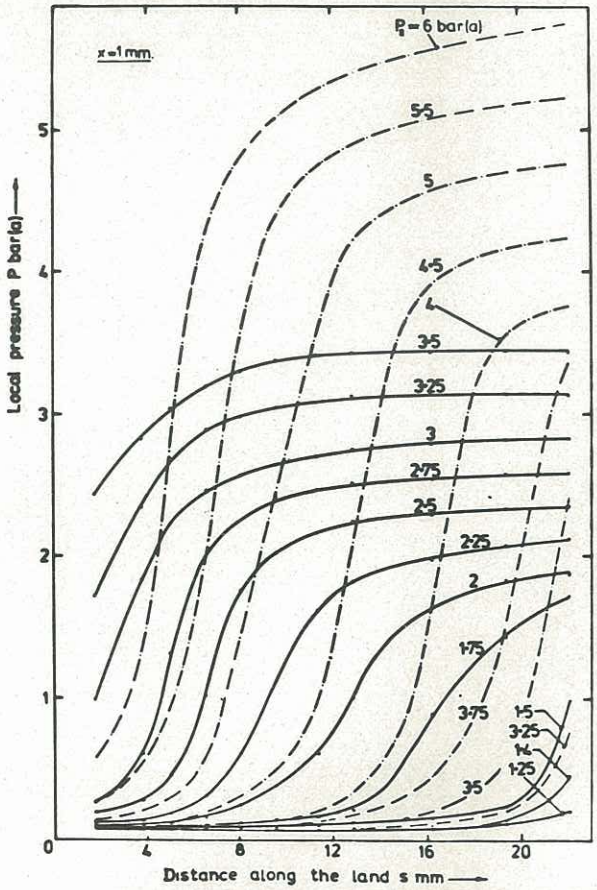


Figure 5 Pressure distribution for different stages of cavitation development. Broken lines are for $P_1$ = 9 bar(a); continuous lines are for 4 bar(a).

## 4 CONCLUSION

It may be concluded that the investigation has enabled one to clarify inception phenomena and to determine for each size of gap the minimum value of the pressure ratio $P_2/P_1$ which must be exceeded if cavitation is to be avoided. The tests also revealed some unexpected aspects of discharge performance when cavitation occurred.

## 5 REFERENCES


LICHTAROWICZ, A. and LORIMER, A.J. (1971). Some flow instabilities in hydraulic restrictions. Proc. Second Fluid Power Symposium (BHRA) pp B1, 1-23.

BIRYUKOV, O.Y. (1974). Cavitation conditions in a jet-screen device operating with back-pressure. Russian Engineering Journal, Vol. 54, pp 19-22.

LICHTAROWICZ, A. and PEARCE, I.D. (1974). Cavitation and aeration effects in long orifices. Proc. I.Mech.E. Conf. on Cavitation, Edinburgh, pp 129-34.